Progress in Reaction Kinetics and Mechanism

ARTICLE

Open Access

https://doi.org/10.48130/prkm-0024-0002

Progress in Reaction Kinetics and Mechanism **2024**, 49: e003

Experimental and kinetic modeling investigation on ignition characteristics of hydrogen: effects of methane co-firing and dilution gas

Xiaojing Tian[1*], Songlin Liu[2], Jun Fang[2], Qiying Zhang[2], Zhenzhen Feng[1] and Qilong Fang[2]

[1] *National Key Laboratory of Clean and Efficient Turbine Power Equipment of Dongfang Turbine Co., Ltd, Dongfang Electric Corporation, Deyang 61800, China*
[2] *School of Mechanical Engineering, Shanghai Jiao Tong University, Shanghai 200240, China*
* Corresponding author, E-mail: tianxiaojing@dongfang.com

Abstract

The large-scale adoption of hydrogen and its co-combustion in gas turbines is critical for achieving carbon neutrality goals. This study examines the ignition characteristics of pure hydrogen and hydrogen-methane blends, with methane content ranging from 0% to 70%, in a shock tube at temperatures between 950–2,100 K and pressures from 1.2 to 5.0 atm. The results show that increasing the methane content leads to longer ignition delay times, indicating a significant reduction in combustion reactivity. A combustion kinetic model for hydrogen and methane was also developed, demonstrating accurate predictions of ignition delay times across various blending ratios, pressures, and temperatures. Rate of production and sensitivity analyses reveal that, compared to pure hydrogen, the addition of methane increases CH_3 radicals while decreasing H radicals. This shift causes methane-driven reactions to dominate, while hydrogen-related reactions weaken. Methane co-firing thus provides flexible control over ignition delay times, offering a direct means to adjust fuel reactivity. CO_2 plays a key role in next-generation gas turbines with hydrogen-enriched blends, oxy-fuel combustion, and combined cycles involving shunt and recompression, all of which contribute to flexible fuel usage, low emissions, and high efficiency. This work also investigates the diluent gas effect of CO_2 on the hydrogen-methane co-firing system. It is revealed that CO_2 affects ignition delay in two key ways: it shortens delay due to its high specific heat capacity, yet it can also lengthen it by competing with H radicals.

Citation: Tian X, Liu S, Fang J, Zhang Q, Feng Z, et al. 2024. Experimental and kinetic modeling investigation on ignition characteristics of hydrogen: effects of methane co-firing and dilution gas. *Progress in Reaction Kinetics and Mechanism* 49: e003 https://doi.org/10.48130/prkm-0024-0002

Introduction

Zero-carbon renewable clean energy is a critical pathway for China to achieve its carbon peaking and carbon neutrality goals, as well as a new driving force for promoting high-quality economic and social development[1]. Hydrogen, as a highly promising zero-carbon energy carrier[2,3], can be produced through clean energy sources such as solar energy and renewable electricity[4–6]. The large-scale utilization of hydrogen in gas turbines is of great significance for realizing the dual carbon targets. However, hydrogen's highly reactive chemical properties, combined with its fast flame propagation speed, make it prone to issues such as flashback and thermoacoustic instabilities, leading to combustion instability in gas turbine systems[7,8]. Methane, the primary component of natural gas, is currently a significant fuel for gas turbines. Co-firing hydrogen with methane can partially replace methane and serve as a key approach to modulate fuel reactivity and facilitate hydrogen utilization. Therefore, it is essential to gain a deeper understanding of the ignition characteristics under both pure hydrogen combustion, and hydrogen-methane co-firing conditions.

Based on shock tubes and rapid compression machines, experimental and modeling studies on the ignition characteristics of hydrogen/methane mixtures have been conducted. These studies primarily focus on the effects of factors such as temperature, pressure, equivalence ratio, and blending ratio on ignition delay times (IDTs). Petersen et al.[9] investigated the ignition characteristics of hydrogen/methane mixtures with methane blending ratios of 20% and 40%. The results indicated that an increase in the methane proportion significantly lengthened the IDTs, while the co-firing of methane did not alter the overall activation energy. Herzler & Naumann[10] measured the IDTs of hydrogen/methane/ethane mixtures with hydrogen content ranging from 0% to 100% under conditions of 900–1,800 K and 1.0–16.0 atm using a shock tube. They also predicted the IDTs using mechanisms such as GRI Mech 3.0[11]. A comparison revealed that mechanisms like GRI Mech 3.0[11] struggled to accurately capture the reduction in activation energy at low temperatures in systems with high hydrogen content. Zhang et al.[12,13] investigated the ignition characteristics of hydrogen/methane mixtures in a shock tube at pressures ranging from 5 to 20 atm, with methane proportions varying from 0% to 100%. The results similarly demonstrated that the ignition temperature of the reaction system increased significantly with the rise in methane proportion. These measurements were used to validate models such as the NUI Galway Mech[11], and USC Mech 2.0[14]. However, the performance of different models in predicting IDTs varied considerably, especially under pure hydrogen conditions. It was thus observed that the current models exhibit significant discrepancies in their predictions for different hydrogen/methane blending ratios, failing to achieve accurate predictions across a broad range of conditions. Donohoe et al.[15] studied the ignition delay times of hydrogen/methane mixtures over various temperatures and pressures using shock tubes, and rapid compression machines. Panigrahy et al.[16] focused on comparing the reaction mechanisms of hydrogen, methane, and hydrogen-methane mixtures across different temperature ranges, explaining the intrinsic mechanism behind the long ignition delay time of hydrogen compared to methane and hydrogen-methane mixtures in the low-temperature regime.

In addition, CO_2 is widely used in combustion processes such as oxy-fuel combustion and exhaust gas recirculation (EGR). The next generation of gas turbines will adopt hydrogen-rich blending, pure oxygen combustion, and Allam cycle technology to achieve flexible

fuel use, low emissions, and high efficiency. In oxy-fuel combustion with carbon-containing fuels, the products are a steam-CO_2 mixture, which allows for high-concentration CO_2 capture through a simple steam condensation and separation process, enabling near-zero CO_2 emissions. Moreover, as the working fluid and fuel are nitrogen-free, this fundamentally eliminates the issue of NOx emissions. Karimi et al.[17] studied the IDTs of syngas in CO_2 and Ar atmospheres. Their kinetic analysis suggested that CO_2 competes with the production of OH radicals. However, contrary to expectations, the experimental results did not reveal any significant difference in IDTs between the CO_2 and Ar atmospheres. The authors attributed this to a combined kinetic effect, but such an explanation is unconvincing. Shao et al.[18] investigated the differences in IDTs of H_2 and CH_4 in 85% CO_2 atmospheres. The model showed good agreement with experimental data at high pressures. However, the sensitivity analysis did not identify any reactions involving CO_2, which contradicts the kinetic analysis by Karimi et al.[17]. Additionally, it is unfortunate that Shao et al.'s study did not compare other dilution atmospheres, making it impossible to determine whether CO_2 had any influence on the experimental results. Subsequently, Harman-Thomas et al.[19] investigated the IDTs of H_2 under varying CO_2/N_2 concentrations. Their findings revealed a significant difference in IDTs between H_2 in CO_2 and N_2 diluted atmospheres. Kinetic analysis demonstrated that CO_2 participates in competition for H radicals, further influencing the ignition delay time of the fuel. In summary, it can be observed that the current research has relatively few studies addressing the impact of CO_2 on the IDTs of CH_4/H_2 fuel mixtures.

In this study, three representative fuel compositions with potential for gas turbine applications were selected for hydrogen/methane mixtures: 100% H_2, 50% H_2/50% CH_4, and 30% H_2/70% CH_4. Under conditions using CO_2 and Ar as diluent gases, the ignition characteristics were investigated using a shock tube at 950–2,100 K, 1.2–5.0 atm, and an equivalence ratio (φ) of 0.5, with IDTs measured under various operating conditions. A kinetic model for H_2/CH_4 combustion under different diluent atmospheres (Ar and CO_2) was constructed and validated using the experimental data. Based on this model, reaction rate analysis and sensitivity analysis were conducted to explore the kinetic mechanisms influencing ignition characteristics under different pressures and blending ratios. This provides foundational data support for the large-scale, stable combustion of hydrogen in gas turbine applications.

Experiment and methods

Measurement of ignition delay times

The experiments in this study were conducted using the shock tube experimental platform at Shanghai Jiao Tong University (Shanghai, China). As shown in (Fig. 1), the platform primarily consists of four components: the shock tube body, the exhaust system, the gas mixing and delivery system, and the signal acquisition system. The shock tube body is constructed from stainless steel, with an inner diameter of 92 mm. The driver section is 3.5 m in length, while the driven section extends 5.5 m. The diaphragm separating the two sections is ruptured using the cross-blade method. The exhaust system consists of three stages: an oil pump, a roots pump, and a molecular pump. The gas mixing and delivery system primarily includes a premix tank and gas cylinders, with the mixture prepared using Dalton's partial pressure method. The gas mixture is left to stand for 12 h to ensure thorough premixing. The signal acquisition system comprises five dynamic pressure sensors located along the driven section, a signal conditioning instrument, a photomultiplier tube (PMT), and a computer for data processing. During the experiment, the shock tube was evacuated stepwise using an oil pump, a roots pump, and a molecular pump. Once the pressure dropped below 3 Pa, the driven and driver sections were filled with gas. He was used as the driver gas. When the pressure difference between the driver and driven sections reached the diaphragm rupture pressure, the polyester diaphragm ruptured, generating an incident shock wave. The pressure jump caused by the incident shock was monitored by dynamic pressure sensors, with the signals converted into voltage through a charge amplifier and signal conditioner. The velocity of the incident shock wave was calculated based on the arrival times at each pressure sensor and the distances between the sensors. The velocity of the reflected shock wave at the tube end was then extrapolated using a linear relationship. The OH emission signal generated during fuel ignition was synchronously recorded by PMT after signal conditioning. The reaction temperature (T5) and pressure (P5) behind the reflected shock wave were calculated using MATLAB, based on the experimental conditions and shock wave properties.

The definition of ignition delay time is illustrated in Fig. 2. To avoid difficulties in determining IDTs under low-temperature conditions, where weak ignition and minimal pressure rise may make IDTs determination unclear, the ignition delay time is uniformly defined as the intersection point between the extrapolated line at the maximum slope of the OH signal and the horizontal baseline. It should be noted that the non-ideal boundary layer effects measured by the change in pressure (dP/dt) behind the reflected shock wave were determined to be less than 4%/ms. The experimental measurement error for IDTs is estimated to be 20%. The fuels used in this study were 100% H_2, 50% H_2/50% CH_4, and 30% H_2/70% CH_4. The mixtures were diluted with 90% Ar, except for case 7, which used 90% CO_2 as the diluent. The equivalence ratio for all cases was set at 0.5. The specific cases are listed in Table 1.

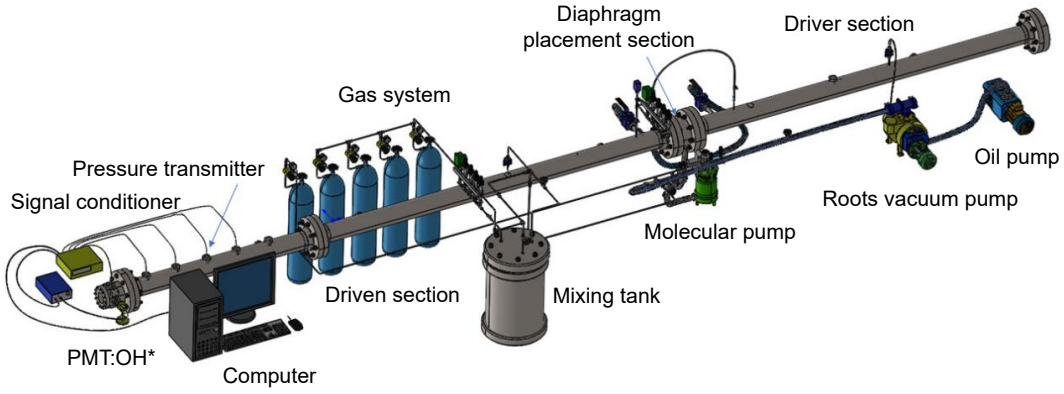

Fig. 1 Schematic diagram of the shock tube system.

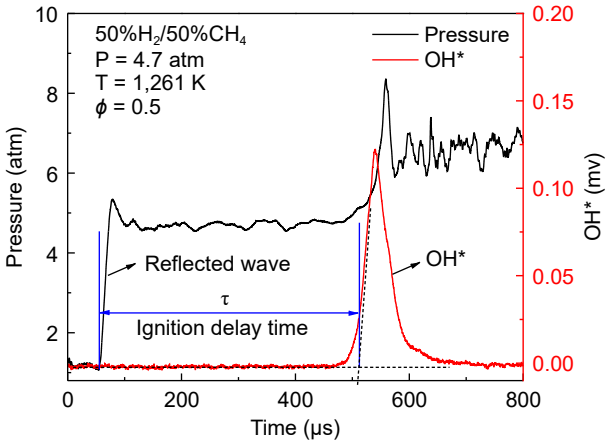

Fig. 2 Definition of ignition delay time.

Reaction kinetic model

Based on the previously developed C0-C4 core combustion reaction mechanism from previous research[20,21], a combustion reaction mechanism for hydrogen and methane (hereafter referred to as SJTU Mech) was developed. The mechanism consists of 43 species and 388 reactions. The hydrogen sub-mechanism is primarily derived from the hydrogen model developed by Hashemi et al. in 2015[22]. The reaction $H+O_2 \rightleftharpoons O+OH$ adopts the reaction rate constants determined by Yu et al.[23] based on shock tube measurements. The methane sub-mechanism is mainly adopted from the methane model developed by Jin et al.[24], which includes methane unimolecular reactions, hydrogen abstraction reactions, and subsequent reactions of CH_3. The rate constants for the reactions $CH_3+H(+M) \rightleftharpoons CH_4(+M)$ and $CH_4+H \rightleftharpoons CH_3+H_2$ are taken from the shock tube measurements by Wang et al.[25] and Srinivasan et al.[26], respectively. Sutherland et al.[27] measured the rate constants for the reaction $CH_4+H \rightleftharpoons CH_3+H_2$ using shock tube laser photolysis coupled with H-atom absorption spectroscopy. The present model adopts their measured results. The rate constants for hydrogen abstraction reactions of methane with O_2, CH_3, and O are taken from GRI Mech 3.0[28] and the evaluations by Baulch et al.[29]. The generated CH_3 can undergo recombination reactions with species such as H and CH_3, as well as oxidation reactions with O_2, O, and HO_2, leading to the formation of formaldehyde. The model also includes the rapid dissociation reaction of HCO proposed by Labbe et al. in 2016[30]. The HCO generated from formaldehyde hydrogen abstraction reactions is highly energetic; part of the HCO de-excites to form stable HCO, while another portion may dissociate rapidly without de-excitation to form CO and H, known as the rapid dissociation of HCO. This reaction facilitates the direct and efficient production of H atoms in formaldehyde hydrogen abstraction, thereby enhancing the reactivity of the combustion system. As a crucial component in technologies such as oxy-fuel combustion, biogas, and flue gas recirculation, CO_2 is an important factor. In this model, the reaction rate constants for the reaction $CO_2+H \rightleftharpoons CO+OH$ were re-evaluated, utilizing the rate constants from the model developed by Zhang et al.[12]. Additionally, this study compares the performance of various core mechanisms, including NUI Galway Mech[11], USC Mech 2.0[14], and GRI Mech 3.0[28], in predicting IDTs. The simulation of IDTs was conducted using the Closed Homogeneous Batched Reactor module of Chemkin-Pro[31].

$$H+O_2 \rightleftharpoons O+OH \quad (R1)$$

$$CH_4+H \rightleftharpoons CH_3+H_2 \quad (R2)$$

$$CH_3+H(+M) \rightleftharpoons CH_4(+M) \quad (R3)$$

Results and discussion

Ignition characteristics of H_2/CH_4 with different blending ratios

Figure 3 presents a comparison of experimental measurements and model predictions of IDTs for 100% H_2, 50% H_2/50%CH_4, and 30% H_2/70% CH_4 under pressures of 1.2 and 5.0 atm. There is a strong linear relationship between IDTs and 1/T when the pressure is 1.2 atm. As the proportion of methane increases, the IDTs curves shift progressively toward higher temperatures. Notably, when the methane content reaches 70%, the ignition temperature significantly increases, and the IDTs also rise sharply. This indicates that an increase in methane proportion reduces the reactivity of the fuel mixture, requiring higher temperatures for ignition, thereby illustrating the ability of methane to flexibly modulate the reactivity of the mixture over a wide range. Furthermore, it can be observed from the figure that at 1.2 atm, the differences among the various models are minimal, all accurately predicting the experimental results.

As the pressure increases, the IDTs curves shift toward the lower temperature region. At a pressure of 5.0 atm, there is a strong linear relationship between IDTs and 1/T under the conditions of 50% CH_4, and 70% CH_4. However, under direct hydrogen combustion conditions, the IDTs curves exhibit significant differences across various temperature ranges. Specifically, IDTs remain relatively low within the temperature range of 1,040–1,250 K, while they increase sharply below 1,040 K, reflecting the highly reactive nature of hydrogen combustion. Under the 5.0 atm condition, different models yield consistent predictions for IDTs in the high-temperature region, but discrepancies arise in the low-temperature region, particularly under direct hydrogen combustion, where the deviations are most pronounced. SJTU Mech demonstrates good predictive performance for experimental results across different conditions. NUI Galway Mech and USC Mech 2.0 are well-developed, thus exhibiting reasonable prediction errors for hydrogen. In contrast, GRI Mech 3.0, primarily developed for methane combustion, shows larger prediction errors under these conditions; however, the predictions improve as the proportion of methane increases. A comprehensive comparison of IDTs results for various hydrogen-to-methane ratios

Table 1. Experimental conditions for the ignition delay time measurements.

No.	Equivalence ratio	$X_{H2}/(X_{H2}+X_{CH4})$	H_2 (%)	CH_4 (%)	O_2 (%)	Dilution gas (%)	Pressure (atm)
1	0.50	1.00	5.00	0.00	5.00	90.00 Ar	1.20
2	0.50	1.00	5.00	0.00	5.00	90.00 Ar	5.00
3	0.50	0.50	1.43	1.43	7.14	90.00 Ar	1.20
4	0.50	0.50	1.43	1.43	7.14	90.00 Ar	5.00
5	0.50	0.30	0.73	1.71	7.56	90.00 Ar	1.20
6	0.50	0.30	0.73	1.71	7.56	90.00 Ar	5.00
7	0.50	0.50	1.43	1.43	7.14	90.00 CO_2	1.20

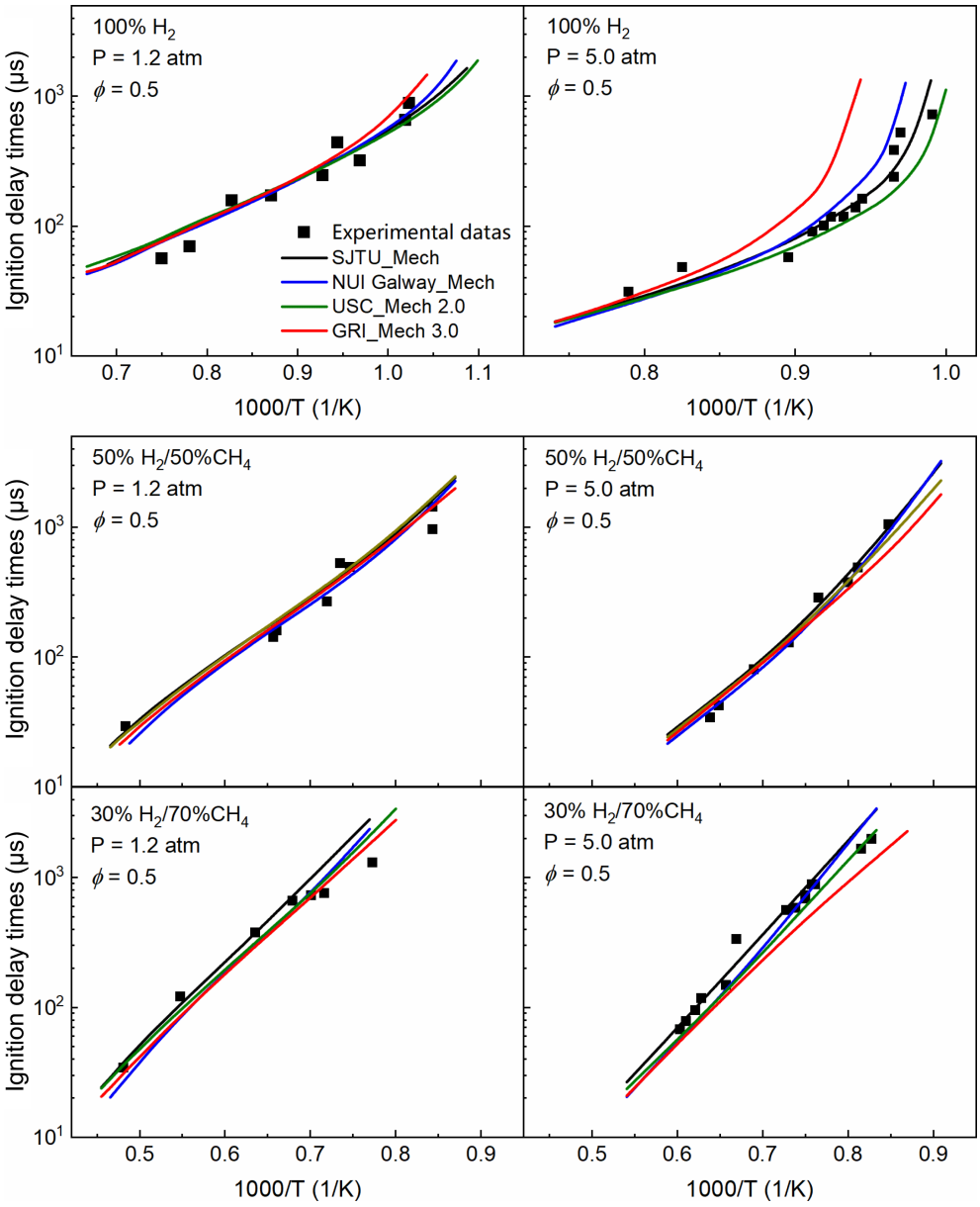

Fig. 3 Comparison of experimental (dots) and simulated (lines) results of IDTs for 100% H_2, 50% H_2/50% CH_4, and 30% H_2/70% CH_4 at 1.2 and 5.0 atm.

indicates that the incorporation of methane allows for flexible adjustment of the reactivity and ignition characteristics of the H_2/CH_4 mixture over a wide range.

To reveal the kinetic mechanisms at different blending ratios, reaction pathway analyses were conducted based on SJTU Mech for two blending ratios: 100% H_2 and 30% H_2/70% CH_4 under conditions of 1,100 K and 5.0 atm, as shown in Fig. 4. For 100% H_2, more than 75% of the hydrogen is directly converted into the stable product H_2O through hydrogen abstraction reactions with OH. A smaller portion of hydrogen is transformed into radicals such as H and OH through oxidation and hydrogen abstraction reactions. Most of the H radicals are further converted into OH radicals, which are ultimately converted into H_2O. It can be observed that hydrogen can directly generate reactive hydrogen atoms through a few reaction sequences, which then undergo chain branching reactions. This explains why hydrogen has high reactivity, ignites easily, and results in shorter IDTs.

For the 30% H_2/70% CH_4 mixture, CH_4 is primarily consumed through hydrogen abstraction reactions with various radicals such as OH, O, and H, leading to the formation of CH_3. Under lean combustion conditions, hydrogen abstraction by OH and O radicals accounts for 85% of methane consumption. CH_3 predominantly undergoes oxidation reactions to further convert into CH_2O, with some forming CH_3O, which almost entirely converts back into CH_2O. CH_2O then undergoes hydrogen abstraction to form HCO, which is gradually converted into CO and CO_2. Thus, CH_3 and CH_2O are the key intermediates in methane combustion.

Comparing the two blending ratios reveals that, in the methane-dominated 30% H_2/70% CH_4 reaction system, the oxidation process led by CH_3 is influenced by hydrogen. Hydrogen provides an abundant supply of OH and H radicals, which accelerates the conversion of CH_4 to CH_3 and further to CO_2. In contrast, in the hydrogen-dominated system, CH_3 does not play a role, and the reaction process is much simpler compared to the system involving methane. The addition of methane alters the reaction pathways, thereby controlling the reaction rate of the mixed fuel system, ensuring stable combustion of hydrogen.

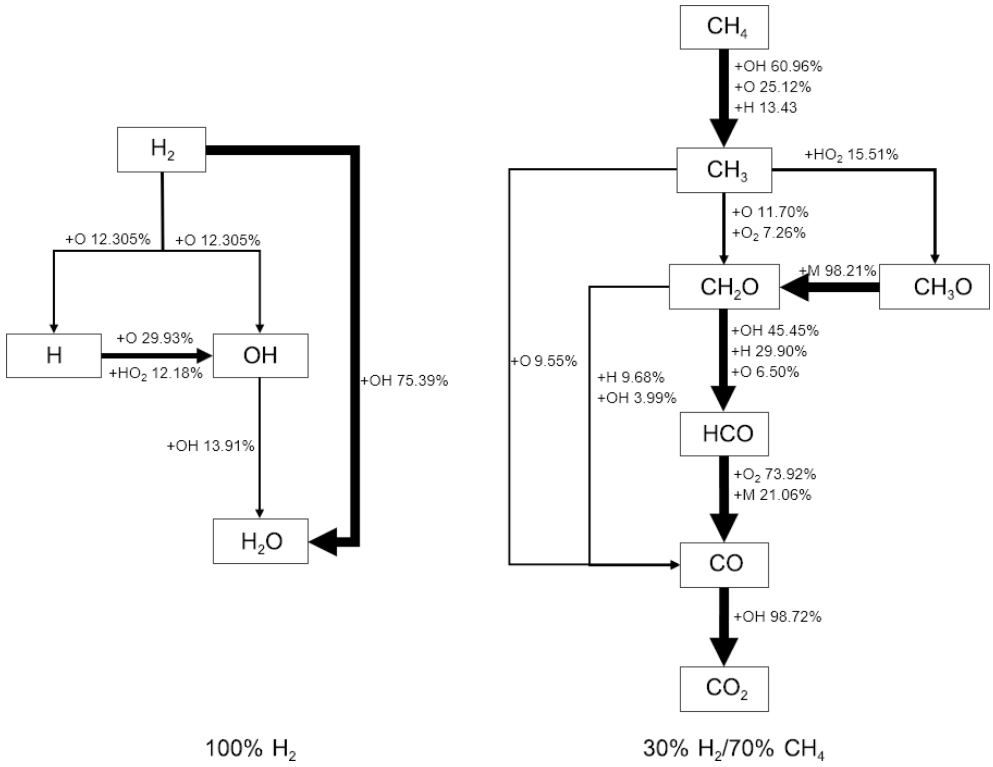

Fig. 4 Reaction pathways of 100% H_2, and 30% H_2/70% CH_4 at 1,100 K, and 5.0 atm.

To investigate the key reactions controlling ignition at different blending ratios, IDTs sensitivity analyses were conducted for 100% H_2, 50% H_2/50% CH_4, and 30% H_2/70% CH_4 under conditions of 1,100 K and 5.0 atm. The sensitivity coefficient is defined as follows[12,13]:

$$S = \frac{\tau(2k_i) - \tau(0.5k_i)}{1.5\tau(k_i)}$$

where, S represents the sensitivity coefficient, τ is the ignition delay time, and k_i is the rate constant of reaction *i*.

The sensitivity analysis results are shown in Fig. 5. It can be observed that for mixtures with different blending ratios, IDTs are consistently influenced by the reaction R1 $H+O_2 \rightleftharpoons O+OH$, which is the most critical chain-branching reaction in the system and significantly promotes ignition, thus exhibiting negative sensitivity. In contrast, reactions with positive sensitivity show greater variability across different blending ratios. For 100% H_2, the reaction R4 $H+O_2(+M) \rightleftharpoons HO_2(+M)$, which competes with R1, is the most important chain-inhibiting reaction in hydrogen combustion, showing the highest positive sensitivity. Additionally, the interconversion reactions between radicals such as H, O, OH, and HO_2 also demonstrate a certain level of sensitivity.

$$H_2+OH \rightleftharpoons H+H_2O \quad (R4)$$

$$CH_3+HO_2 \rightleftharpoons CH_3O+OH \quad (R5)$$

$$CH_3+O_2 \rightleftharpoons CH_2O+OH \quad (R6)$$

$$CH_4+OH \rightleftharpoons CH_3+H_2O \quad (R7)$$

$$H+O_2(+M) \rightleftharpoons HO_2(+M) \quad (R8)$$

$$CH_3+CH_3(+M) \rightleftharpoons C_2H_6(+M) \quad (R9)$$

$$CH_3+HO_2 \rightleftharpoons CH_4+O_2 \quad (R10)$$

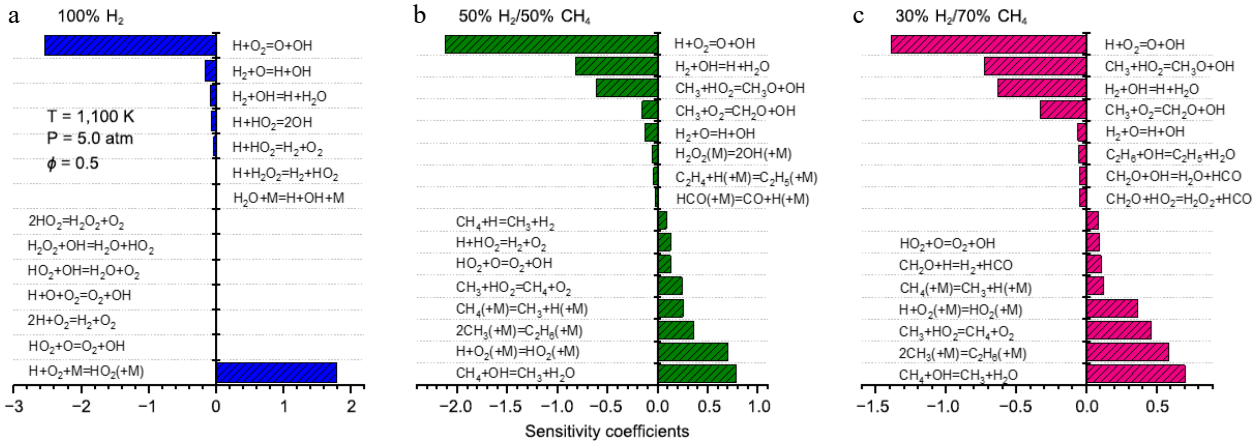

Fig. 5 Sensitivity analysis of IDTs for 100% H_2, 50% H_2/50% CH_4, and 30% H_2/70% CH_4 under conditions of 1,100 K and 5.0 atm.

$$C_2H_6+OH \rightleftharpoons C_2H_5+H_2O \quad (R11)$$

As the methane proportion increases to 50%, in addition to the reactions mentioned above, methane combustion-related reactions begin to appear among the sensitive reactions. Particularly, reactions involving CH_3, such as R5 $CH_3+HO_2 \rightleftharpoons CH_3O+OH$, R6 $CH_3+O_2 \rightleftharpoons CH_2+OH$, R7 $CH_4+OH \rightleftharpoons CH_3+H_2O$, R9 $CH_3+CH_3(+M) \rightleftharpoons C_2H_6(+M)$, R3 $CH_4(+M) \rightleftharpoons CH_3+H(+M)$, and R10 $CH_3+HO_2 \rightleftharpoons CH_4+O_2$ become significant.

For ignition-promoting reactions, in addition to the dominant role of R1, reaction R4 $H_2+OH \rightleftharpoons H+H_2O$ is also an important chain propagation reaction that produces reactive H radicals, with a sensitivity coefficient higher than that under 100% H_2 conditions. Reactions R5 and R6 also exhibit significant negative sensitivity. Among the positive sensitivity reactions, the chain-inhibiting reaction R7 converts active OH radicals into less reactive CH_3, replacing R8 as the dominant inhibiting reaction for the 50% H_2/50% CH_4 mixture, with a slightly higher sensitivity coefficient than R8. Reactions R9, R3, and R10 are chain-terminating reactions in the methane combustion process, with R9 and R3 being pressure-dependent reactions that demonstrate higher sensitivity under elevated pressures. Reaction R9 consumes radicals through the combination of two CH_3 species, thus inhibiting the ignition process, while reaction R3 suppresses ignition by consuming H and CH_3. As the proportion of methane increases to 70%, the sensitivity of the carbon-involved reactions continues to enhance, as seen in R5, R6 $CH_3+O_2 \rightleftharpoons CH_2O+OH$, R11 $C_2H_6+OH \rightleftharpoons C_2H_5+H_2O$. At this point, methane combustion gradually becomes the controlling mechanism of the system. In terms of inhibition reactions, chain-inhibiting reactions R7, R9, and R10, which are dominated by methane, begin to take precedence, while the chain-inhibiting reaction R8, which is primarily influenced by hydrogen, gradually diminishes.

Figure 6 compares the peak concentrations of key radicals H, O, OH, and CH_3 in 100% H_2 and 50% H_2/50% CH_4. From the figure, it is clear that in the 100% H_2 case, the concentrations of H, O, and OH radicals are relatively high, with no production of CH_3. This indicates a strong ability to produce hydrogen atoms, reflecting the effectiveness of the chain-branching reaction R1. In contrast, in the 50% H_2/50% CH_4 mixture, the concentration of H atoms decreases sharply, while a certain amount of CH_3 is formed. CH_3 tends to consume active radicals, which together lead to a decrease in system activity, causing the IDTs to become longer.

Dilution gas effect

In oxy-fuel combustion and biogas combustion, there is a significant amount of CO_2, which can have a noticeable impact on the IDTs of the fuel. The influence of CO_2 and Ar on the ignition delay time of a 50% H_2/50% CH_4 mixture is shown in Fig. 7. From the figure, it can be observed that CO_2 significantly increases the IDTs, indicating a negative effect on the ignition of the fuel mixture. Additionally, when the temperature drops below 1,538 K, the mixture does not ignite in the presence of CO_2, whereas Ar allows the mixture to ignite over a broader temperature range and has minimal impact on the IDTs. This difference can be attributed to two main factors. First, CO_2 has a higher specific heat capacity, causing it to absorb more heat after the reflected shockwave reaches the fuel, slowing down the temperature increase and thus affecting the ignition temperature. Second, CO_2 may also participate in chemical reaction pathways at high temperatures, further influencing the combustion process.

The sensitivity analysis of IDTs for a 50% H_2/50% CH_4 mixture at 1,600 K in a high CO_2 environment is shown in Fig. 8. Under high CO_2 conditions, the main ignition-promoting reactions remain R1 and R4, which continue to play dominant roles. However, for inhibition reactions, the leading reactions shift from R7 and R8 (under argon conditions) to R7 and R12 in the presence of CO_2. From reaction R12, it can be observed that CO_2 directly participates in the reaction with H radicals, rather than just acting through collision

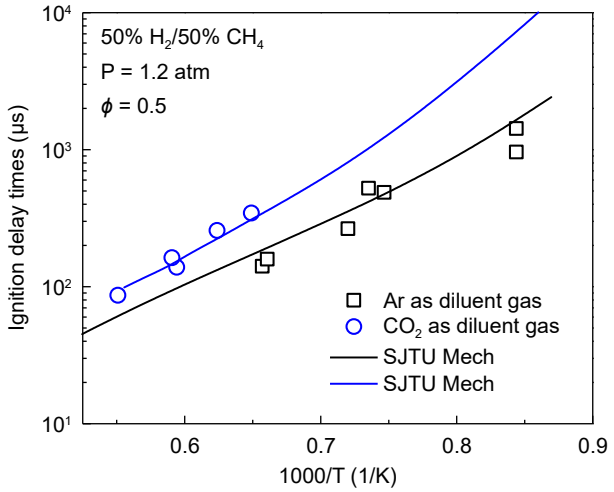

Fig. 7 Effect of CO_2 on ignition delay times of 50% H_2/50% CH_4 mixture.

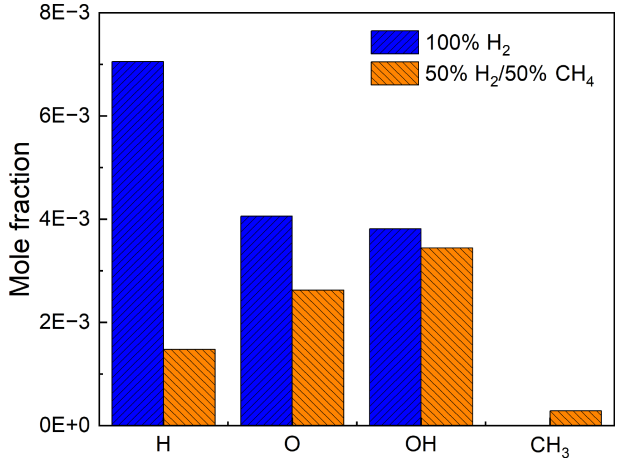

Fig. 6 Peak concentrations of H, O, OH, and CH_3 radicals at 1,100 K and 5.0 atm for 100% H_2 and 50% H_2/50% CH_4.

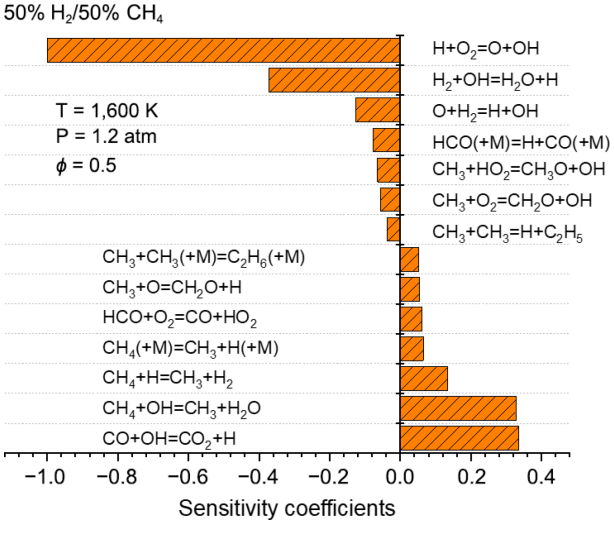

Fig. 8 Sensitivity coefficients of IDTs under CO_2 atmosphere.

effects. CO_2 competes with O_2 for H radicals, weakening the chain-branching effect of reaction R1, which leads to extended IDTs and reduces the reactivity of the fuel.

$$CO+OH \rightleftharpoons CO_2+H \quad (R12)$$

Conclusions

This study conducted shock tube experiments and kinetic modeling to investigate the ignition characteristics of hydrogen combustion and hydrogen/methane co-combustion. The main conclusions are as follows:

(1) The IDTs of pure hydrogen remain low within the temperature range of 1,040–1,250 K, but it increases sharply at temperatures below 1,040 K. As the methane proportion increases, the IDTs curve shifts toward higher temperatures. When the fuel contains 70% methane, the ignition temperature significantly rises, and IDTs increase substantially. With increasing pressure, the IDTs curve shifts to lower temperatures, resulting in shorter IDTs. Comparing the IDTs results for different methane blending ratios indicates that hydrogen/methane co-combustion allows flexible adjustment of IDTs and the reactivity of the hydrogen fuel over a wide range.

(2) Different kinetic models perform well in predicting IDTs at atmospheric pressure for varying methane blending ratios. However, at 5.0 atm in relatively low-temperature regions, noticeable differences arise, particularly under pure hydrogen conditions. SJTU Mech, NUI Galway Mech, and USC Mech 2.0 models generally show better agreement with experimental data.

(3) Compared to pure hydrogen combustion, the addition of methane increases the concentration of radicals such as CH_3 and decreases the concentration of radicals like H. This shift allows methane-dominated reactions to take control, particularly reactions such as R7 $CH_4+OH \rightleftharpoons CH_3+H_2O$ and R8 $CH_3+CH_3(+M) \rightleftharpoons C_2H_6(+M)$, while hydrogen-dominated reactions are weakened.

(4) CO_2 has a significant effect on ignition delay time. It directly participates in the reaction with H radicals and competes with O_2 for H radicals, thereby weakening the promoting effect of reaction R1. This results in increased IDTs and reduced reactivity of the fuel mixture.

Author contributions

The authors confirm contribution to the paper as follows: conceptualization: Tian X; formal analysis: Tian X, Feng Z; investigation: Tian X, Liu S, Fang J, Zhang Q, Fang Q; writing - original draft preparation: Tian X; writing - review & editing: Liu S. All authors reviewed the results and approved the final version of the manuscript.

Data availability

All data generated or analyzed during this study are included inthis published article.

Acknowledgments

The research was supported by the fund of State Key Laboratory of Long-life High Temperature Materials (DEC8300CG202210287EE280292).

Conflict of interest

The authors declare that they have no conflict of interest.

Dates

Received 19 October 2024; Revised 25 November 2024; Accepted 27 November 2024; Published online 30 December 2024

References

1. Teng X, Zhuang W, Liu FP, Chang TH, Chiu YH. 2023. China's path of carbon neutralization to develop green energy and improve energy efficiency. *Renewable Energy* 206:397–408
2. Hassan Q, Sameen AZ, Salman HM, Jaszczur M, Al-Jiboory AK. 2023. Hydrogen energy future: Advancements in storage technologies and implications for sustainability. *Journal of Energy Storage* 72:108404
3. Le TT, Sharma P, Bora BJ, Tran VD, Truong TH, et al. 2024. Fueling the future: A comprehensive review of hydrogen energy systems and their challenges. *International Journal of Hydrogen Energy* 54:791–816
4. Dermühl S, Riedel U. 2023. A comparison of the most promising low-carbon hydrogen production technologies. *Fuel* 340:127478
5. El-Shafie M. 2023. Hydrogen production by water electrolysis technologies: A review. *Results in Engineering* 20:101426
6. Zhang L, Jia C, Bai F, Wang W, An S, et al. 2024. A comprehensive review of the promising clean energy carrier: Hydrogen production, transportation, storage, and utilization (HPTSU) technologies. *Fuel* 355:129455
7. Halter F, Chauveau C, Djebaïli-Chaumeix N, Gökalp I. 2005. Characterization of the effects of pressure and hydrogen concentration on laminar burning velocities of methane–hydrogen–air mixtures. *Proceedings of the Combustion Institute* 30:201–08
8. Ilbas M, Crayford AP, Yılmaz İ, Bowen PJ, Syred N. 2006. Laminar-burning velocities of hydrogen–air and hydrogen–methane–air mixtures: An experimental study. *International Journal of Hydrogen Energy* 31:1768–79
9. Petersen EL, Hall JM, Smith SD, de Vries J, Amadio AR, et al. 2007. Ignition of Lean Methane-Based Fuel Blends at Gas Turbine Pressures. *Journal of Engineering for Gas Turbines and Power* 129:937–44
10. Herzler J, Naumann C. 2009. Shock-tube study of the ignition of methane/ethane/hydrogen mixtures with hydrogen contents from 0% to 100% at different pressures. *Proceedings of the Combustion Institute* 32:213–20
11. Petersen EL, Kalitan DM, Simmons S, Bourque G, Curran HJ, et al. 2007. Methane/propane oxidation at high pressures: Experimental and detailed chemical kinetic modeling. *Proceedings of the Combustion Institute* 31:447–54
12. Zhang Y, Huang Z, Wei L, Zhang J, Law CK. 2012. Experimental and modeling study on ignition delays of lean mixtures of methane, hydrogen, oxygen, and argon at elevated pressures. *Combustion and Flame* 159:918–31
13. Zhang Y, Jiang X, Wei L, Zhang J, Tang C, et al. 2012. Experimental and modeling study on auto-ignition characteristics of methane/hydrogen blends under engine relevant pressure. *International Journal of Hydrogen Energy* 37:19168–76
14. Wang H, You XQ, Joshi AV, Davis SG, Laskin A, et al. 2007. USC Mech Version II. High-temperature combustion reaction model of H2/CO/C1-C4 compounds. http://ignis.usc.edu/USC_Mech_II.htm
15. Donohoe N, Heufer A, Metcalfe WK, Curran HJ, Davis ML, et al. 2014. Ignition delay times, laminar flame speeds, and mechanism validation for natural gas/hydrogen blends at elevated pressures. *Combustion and Flame* 161:1432–43
16. Panigrahy S, Mohamed AAES, Wang P, Bourque G, Curran HJ. 2023. When hydrogen is slower than methane to ignite. *Proceedings of the Combustion Institute* 39:253–63
17. Karimi M, Ochs B, Sun W, Ranjan D. 2021. High pressure ignition delay times of H_2/CO mixture in carbon dioxide and argon diluent. *Proceedings of the Combustion Institute* 38:251–60
18. Shao J, Choudhary R, Davidson DF, Hanson RK, Barak S, Vasu S. 2019. Ignition delay times of methane and hydrogen highly diluted in carbon dioxide at high pressures up to 300 atm. *Proceedings of the Combustion Institute* 37:4555–62

19. Harman-Thomas JM, Kashif TA, Hughes KJ, Pourkashanian M, Farooq A. 2023. Experimental and modelling study of hydrogen ignition in CO_2 bath gas. *Fuel* 334:126664
20. Zhang X, Lailliau M, Cao C, Li Y, Dagaut P, et al. 2019. Pyrolysis of butane-2,3-dione from low to high pressures: implications for methyl-related growth chemistry. *Combustion and Flame* 200:69–81
21. Zhang X, Wang G, Zou J, Li Y, Li W, et al. 2017. Investigation on the oxidation chemistry of methanol in laminar premixed flames. *Combustion and Flame* 180:20–31
22. Hashemi H, Christensen JM, Gersen S, Glarborg P. 2015. Hydrogen oxidation at high pressure and intermediate temperatures: Experiments and kinetic modeling. *Proceedings of the Combustion Institute* 35:553–60
23. Yu CL, Frenklach M, Masten DA, Hanson RK, Bowman CT. 1994. Reexamination of shock-tube measurements of the rate coefficient of $H + O_2 \rightarrow OH + O$. *The Journal of Physical Chemistry* 98:4770–71
24. Jin H, Frassoldati A, Wang Y, Zhang X, Zeng M, et al. 2015. Kinetic modeling study of benzene and PAH formation in laminar methane flames. *Combustion and Flame* 162:1692–711
25. Wang S, Davidson DF, Hanson RK. 2016. Improved shock tube measurement of the $CH_4 + Ar = CH_3 + H + Ar$ rate constant using UV cavity-enhanced absorption spectroscopy of CH_3. *The Journal of Physical Chemistry A* 120:5427–34
26. Srinivasan NK, Su MC, Sutherland JW, Michael JV. 2005. Reflected Shock Tube Studies of High-Temperature Rate Constants for $CH_3 + O_2$, $H_2CO + O_2$, and $OH + O_2$. *The Journal of Physical Chemistry A* 109:7902–14
27. Sutherland JW, Su MC, Michael JV. 2001. Rate constants for $H + CH_4$, $CH_3 + H_2$, and CH_4 dissociation at high temperature. *International Journal of Chemical Kinetics* 33:669–84
28. Smith GP, Golden DM, Frenklach M. n.d. *GRI-Mech 3.0*. www.me.berkeley.edu/gri_mech/version30/text30.html
29. Baulch DL, Bowman CT, Cobos CJ, Cox RA, Just T, et al. 2005. Evaluated Kinetic Data for Combustion Modeling: Supplement II. *Journal of Physical and Chemical Reference Data* 34:757–1397
30. Labbe NJ, Sivaramakrishnan R, Goldsmith CF, Georgievskii Y, Miller JA, et al. 2016. Weakly bound free radicals in combustion: "Prompt" dissociation of formyl radicals and its effect on laminar flame speeds. *The Journal of Physical Chemistry Letters* 7:85–89
31. CHEMKIN-PRO 15092. 2009. *Reaction Design*. San Diego, USA.www.reactiondesign.com/products/chemkin (Retrieved 2015, 4)